Proteomic Investigation of the Signal Transduction Pathways Controlling Colistin Resistance in *Klebsiella pneumoniae*.

Ching Hei Phoebe Cheung[a], Punyawee Dulyayangkul[a], Kate J. Heesom[b], Matthew B. Avison[a]#

[a]School of Cellular & Molecular Medicine, University of Bristol, Bristol. UK

[b] University of Bristol Proteomics Facility, Bristol, UK

#Correspondence to: School of Cellular & Molecular Medicine, University of Bristol, Bristol, United Kingdom. bimba@bris.ac.uk

Running Title: Colistin resistance in *K. pneumoniae*.

Abstract

Colistin resistance in *Klebsiella pneumoniae* is predominantly caused by mutations that increase expression of the *arn* (also known as *pbg* or *pmrF*) operon. Expression is activated by the PhoPQ and PmrAB two-component systems. Constitutive PhoPQ activation occurs directly by mutation or following loss of MgrB. PhoPQ may also cross-activate PmrAB via the linker protein PmrD. Using proteomics, we show that MgrB loss causes a wider proteomic effect than direct PhoPQ activation, suggesting additional targets for MgrB. Different *mgrB* mutations cause different amounts of Arn protein production, which correlated with colistin MIC. Disruption of *phoP* in an *mgrB* mutant had a reciprocal effect to direct activation of PhoQ in a wild-type background, but the regulated proteins showed almost total overlap. Disruption of *pmrD* or *pmrA* slightly reduced Arn protein production in an *mgrB* mutant, but production was still high enough to confer colistin resistance; disruption of *phoP* conferred wild-type Arn production and colistin MIC. Activation of PhoPQ directly, or through *mgrB* mutation did not significantly activate PmrAB or PmrC production but direct activation of PmrAB by mutation did, and also activated Arn production and conferred colistin resistance. There was little overlap between the PmrAB and PhoPQ regulons. We conclude that under the conditions used for colistin susceptibility testing, PhoPQ-PmrD-PmrAB cross-regulation is not significant and that independent activation of PhoPQ or PmrAB is the main reason that Arn protein production increases above the threshold required for colistin resistance.

Introduction

Colistin is increasingly used to treat infections caused by extensively drug resistant Gram-negative bacteria (1). Colistin resistance in carbapenem-resistant *Klebsiella pneumoniae*, which was first reported in 2010 (2-4) is, therefore, a critically important problem. It can be caused by mobile *mcr* genes but by far the most common causes are chromosomal mutations (5,6). For example, loss-of-function mutations in *mgrB* regularly emerge following colistin therapy in the clinic, and when selecting resistant mutants in the laboratory (7-10). Loss of MgrB causes activation of *arn* operon expression (7). This operon, also referred to as the *pbg* or *pmrF* operon (5) encodes a series of enzymes forming a pathway that modifies lipid A in lipopolysaccharide by adding 4-amino-4-deoxy-L-arabinose. This modification has been seen in colistin resistant *K. pneumoniae* mutants in many studies (e.g. 11-13). Its effect is to reduce cell surface negative charge, reducing affinity for positively charged colistin, raising its MIC (5).

Activation of *arn* operon transcription in *K. pneumoniae* involves two upstream promoters, each targeted by a two-component system response regulator. PhoP targets promoter 1 in response to low magnesium concentrations and PmrA targets promoter 2 in response to high iron concentrations and low pH (14). The dramatic impact that cations and pH have on *arn* promoter activity explains the wide range of medium-dependent colistin MICs observed in the laboratory (15,16). According to a joint CLSI and EUCAST report, colistin susceptibility testing needs to be tightly standardised, therefore, and the gold standard is broth microdilution using colistin sulphate, cation adjusted Muller Hinton broth and with no additives (17)

Additional complexity arises in control of *arn* operon transcription in *K. pneumoniae* because the response regulator PhoP can also activate transcription of *pmrD* and PmrD binds PmrA and enhances its activation (14,18). Hence, when low magnesium and high iron occur at the

same time, the PmrA-targeted *arn* operon promoter 2 is more strongly activated than it is in the presence of high magnesium and high iron (14).

The cognate sensor kinases activating PhoP and PmrA are PhoQ and PmrB, respectively (14). It is generally accepted that loss-of-function mutations in *mgrB* activate *arn* operon transcription in *K. pneumoniae* because MgrB is a direct negative regulator of PhoQ sensor kinase activity (5). In fact, this is experimentally confirmed only in *Salmonella* spp. (19) but loss of MgrB does constitutively activate PhoPQ in *K. pneumoniae*, leading to constitutively enhanced transcription from *arn* operon promoter 1 (14). Specific mutations in PhoPQ also activate *arn* operon transcription and confer colistin resistance or heteroresistance in *K. pneumoniae*, e.g. PhoQ substitutions Asp434Asn (20) or Ala21Ser (21) or PhoP substitution Asp191Tyr (22).

Mutations in PmrAB, constitutively activating *arn* operon transcription from promoter 2 have also been found to cause colistin resistance in *K. pneumoniae*. For example, Leu82Arg (23) or Thr157Pro (24) in PmrB, but activation of PmrAB also increases expression of *pmrC*. This encodes an enzyme that modifies lipopolysaccharide by decorating it with phosphoethanolamine, which contributes to colistin resistance in *Salmonella* spp. because it is another way to reduce negative charge on the cell surface (25).

A third two-component regulatory system known to be involved in colistin resistance in *K. pneumoniae* is CrrAB. Activatory mutations in the sensor kinase CrrB have been identified in colistin resistant clinical isolates (20,26,27). Based on transcriptomic analysis these mutants have increased *arn* operon and *pmrC* transcription (20) and in this they closely resemble PmrAB activatory mutants and indeed *pmrAB* is essential for the activation of *arn* operon and *pmrC* transcription in CrrAB activatory mutants, suggesting direct linkage between these two-component systems (26). One additional effect of CrrAB activation is upregulation of *crrC* transcription (20) and *crrC* is also essential for activation of *arn* operon and *pmrC* transcription in a CrrAB activatory mutant (26). This suggests that CrrC forms the link

between activated CrrAB and activation of PmrAB, leading to colistin resistance, but the mechanism by which this link operates is not yet known.

The complexity associated with acquisition of colistin resistance in *K. pneumoniae*, means that clinical cases involve a wide range of mutations. In a recent large clinical survey, *mgrB* loss-of-function was the most common mechanism, but in many cases, additional mutations in two-component system genes was seen, and in cases where multiple mutations were seen, a sequential increase in colistin MIC was observed (28)

The aim of the work reported here was to use LC-MS/MS shotgun proteomics and targeted mutagenesis to investigate the importance of the MgrB-PhoPQ-PmrD-PmrAB signal transduction pathway to modulate Arn protein and PmrC production, and assess the protein abundance thresholds required for colistin resistance in *K. pneumoniae* stimulated by mutations affecting PhoPQ and/or PmrAB activity.

Results and Discussion

The direct role of PhoPQ and the indirect role of signal transduction from PhoPQ through PmrD to PmrAB in Arn protein production and colistin resistance caused by mgrB mutation.

A collection of six *K. pneumoniae* spontaneous single-step mutants were selected in the laboratory using Muller-Hinton agar containing 32 $\mu g.mL^{-1}$ of colistin, and in each case, PCR sequencing confirmed mutation in *mgrB* or upstream. Three different mutations were seen, causing the following changes: Gln29STOP in MgrB (found in four colistin resistant mutants here, represented by mutant P21); an A to G transition at -31 relative to the *mgrB* start codon, weakening a putative second -10 promoter sequence (**Figure 1**) (represented by mutant P22); a deletion comprising the region between -19 relative to the start codon, to remove the first 41 amino acids of MgrB (represented by mutant P23).

Colistin MICs against these three representative mutants were determined and, in all cases, colistin resistance was confirmed (**Table 1**). Envelope proteomics identified 45 proteins significantly differentially regulated in all three *mgrB* mutants relative to the parent strain, Ecl8 (33 up- and 12 down-regulated; **Table 2**). These included the ArnABCDT operon proteins known to be responsible for modification of lipopolysaccharide by the addition of 4-amino-4-deoxy-L-arabinose (5). **Figure 2** shows that Arn protein production is highest in the mutant P23, where MgrB is entirely lost. The *mgrB* nonsense mutant truncated at 29 amino acids, P22 and the *mgrB* promoter mutant P21 both have significantly lower Arn protein production than in P23, implying some residual repressive activity of MgrB in both cases. Overall, P22 had the lowest Arn protein production of the three (**Figure 2**). Nonetheless all three mutants are colistin resistant though, as expected based on Arn protein production levels, the highest MIC is against P23 and the lowest against P22 (**Table 1**). This leads to the conclusion that once Arn protein production increases above a certain threshold, colistin resistance is conferred, but that as protein production increases further – P23>P21>P22 – MIC also increases.

It has been proposed that *arn* operon gene expression is increased upon *mgrB* mutation through activation of the two-component system PhoPQ, and that in addition, there is a secondary increase through activation of the PmrAB two-component system, with PmrD being necessary for transducing PhoPQ activation into PmrAB activation (reviewed in ref. 5). Using *mgrB* mutant P23 as a starting point, we disrupted *phoP*, *pmrD* and *pmrA*, to test the effects of these mutations on Arn protein production and colistin MIC.

Observed Arn protein abundance changes in these regulatory mutants demonstrated the primacy of PhoPQ activation in colistin resistance driven by *mgrB* loss. Arn protein abundance returned to wild-type (**Figure 3**) and colistin MIC fell below the resistance breakpoint (**Table 1**) upon disruption of *phoP* in the *mgrB* mutant P23. In contrast, our proteomics analysis (**Figure 3**) showed that PmrD and PmrAB play only a minor role in increased Arn protein production seen in an *mgrB* mutant. Only ArnC significantly reduced in

abundance following disruption of *pmrA*. There was a larger effect following disruption of *pmrD* (4/5 Arn proteins significantly reduced in abundance) but in neither mutant did any of the Arn proteins fall in abundance significantly below levels seen in the *mgrB* mutants P21 and P22 (**Figure 2**) and not surprisingly therefore, the *pmrA* and *pmrD* mutant derivatives of *mgrB* mutant P23 remained colistin resistant, and the MIC against them was only one doubling dilution below that against P23 (**Table 1**). These data add support for our conclusion that there is a threshold of Arn protein abundance required for colistin resistance. It seems clear that PhoPQ activation alone can support an abundance above this threshold even without any additional effects caused by PmrAB activation.

PhoPQ regulated proteins identified following mgrB mutation and PhoQ activation.

Of 45 proteins (i.e. including the Arn proteins) differentially regulated in all three *mgrB* mutants (**Table 2**) 18 of those upregulated in the *mgrB* mutant P23 returned to wild-type levels upon disruption of *phoP* (**Table 3**). These included the five Arn proteins, the response regulator PhoP itself, LpxO, two Mg^{2+} transporters including MgtA, SlyB and MacA. Transcripts representing all these proteins have been seen to be upregulated in *mgrB* loss-of-function and in PhoQ activatory (PhoQ*) colistin resistant clinical isolates relative to colistin susceptible control isolates through transcriptomics (20). Our proteomics analysis reinforces the definition of a core PhoPQ regulon, but a secondary observation is that the majority (27/45) of the protein abundance changes seen in the *mgrB* mutant P23 do not occur via activation of PhoPQ; they were not reversed following disruption of *phoP* (**Table 3**). The implication of this finding, made here by comparing otherwise isogenic pairs of strains, is that MgrB interacts with regulatory networks other than PhoPQ in *K. pneumoniae*, though these additional effects are not important for colistin resistance, which was completely reversed following disruption of *phoP* (**Table 1**).

In order to further investigate the role of direct PhoPQ activation in colistin resistance, we turned to a colistin resistant, PhoQ* (activatory) mutant that we selected from *K. pneumoniae* clinical isolate KP47 (**Table 1**). Whole genome sequencing identified the mutation causes a Tyr89Asn change in PhoQ. Proteomics comparing KP47 with the PhoQ* mutant derivative revealed that levels of Arn protein production in the PhoQ* mutant were not significantly different from those in the *mgrB* loss-of-function mutant P23 (**Figure 4**). Indeed, despite starting with a different parent strain, significant upregulation of 15/18 proteins seen to become downregulated when *phoP* was disrupted in the Ecl8-derived *mgrB* mutant P23 were also upregulated in the PhoQ* mutant relative to its parent, KP47. This further focussed down onto the core *K. pneumoniae* PhoPQ regulon, which is shown in **Table 3**.

Proteins upregulated following activation of PmrAB.

Disruption of *pmrA* had little effect on Arn protein production in the *mgrB* mutant P23 (**Figure 3**) suggesting that PmrAB activation is not a major cross-regulatory effect of *mgrB* loss in the context of colistin resistance. Nonetheless, it has been reported that PmrAB activation directly by mutation can confer colistin resistance (23,24) and indeed, we were able to select a colistin resistant mutant of clinical isolate KP47 with an activatory mutation in PmrB (**Table 1**). The mutation identified using whole genome sequencing was Thr157Pro. Arn protein abundance in this PmrB* mutant was significantly elevated relative to KP47 in all cases except for ArnB. For all except ArnA and ArnB the extent of abundance increase was like that seen in the PhoQ* derivative of KP47, and the *mgrB* mutant P23 (**Figure 4**). The fact that ArnB abundance did not increase significantly above the level seen in wild-type KP47 was surprising since the PmrB* mutant is colistin resistant, but it was notable that the MIC of colistin against this PmrB* mutant was one doubling dilution below that against the PhoQ* mutant (**Table 1**). This suggested that either significant upregulation of ArnB is not essential for colistin resistance or there is another mechanism involved in colistin resistance in the PmrB* mutant. In total, only 7/45 proteins significantly up- or down-regulated in the *mgrB*

194 mutant P23 were significantly up- or down-regulated in the PmrB* mutant. As well as the Arn
195 proteins (except ArnB), these were SlyB, LpxO and one Mg^{2+} transporter, which are all part
196 of the core PhoPQ regulon (**Table 2**). Transcripts representing all seven of these
197 PrmAB/PhoPQ dual regulated proteins, plus ArnB have also been seen to be upregulated in
198 clinical isolates with activatory mutations in CrrB (20, **Table 2**) which indirectly activates
199 PmrAB (26,27). In search of an additional mechanism of colistin resistance in the PmrB*
200 mutant we searched the 65 proteins differentially regulated in the PmrB* mutant relative to
201 KP47. Three of those most strongly over-produced were PmrA, PmrB and PmrC (**Figure 5**).
202 Transcription of *pmrC* (also known as *eptA*) is known to be positively controlled by PmrAB in
203 *K. pneumoniae* (24). In *Salmonella* spp. it encodes a phosphoethanolamine transferase,
204 responsible for modifying lipopolysaccharide by decorating it with phosphoethanolamine
205 (25). Importantly, we did not see PmrA, B or C upregulation above our limit of detection
206 (around 100 times less than the level seen in the PmrB* mutant) in any *mgrB* loss-of-function
207 mutant or in the PhoQ* mutant (**Figure 5**). These findings fit, therefore, with our conclusion
208 that cross activation of PmrAB (the direct regulator of *pmrC*) following activation of PhoPQ is
209 very limited under the growth conditions used for our analysis. We also conclude that the
210 PmrAB regulon has limited components that overlap with the PhoPQ regulon, and that
211 PmrC, in terms of functionally important protein product upregulation, is unique to the
212 PmrAB-mediated branch of the colistin resistance-mediating regulatory system. This may
213 well explain why, of multiple studies monitoring the impact of *mgrB* loss-of-function on
214 lipopolysaccharide modification in *K. pneumoniae* (11-13,29) only one has reported elevated
215 levels of phosphoethanolamine modification (29). Indeed, even in this case, contrary to
216 expectations, the observed modification, and the observed upregulation of *pmrC* expression
217 were apparently dependent on PhoPQ but not PmrAB, suggesting it was not caused by
218 PhoPQ-PmrD-PmrAB cross-regulation at all (29). Furthermore, the authors showed that
219 *pmrC* disruption in an *mgrB* loss-of-function mutant background only had a small impact on
220 survival in the presence of colistin (29). This implies that even when rarely seen,
221 phosphoethanolamine modification by PmrC has only a minor role in colistin resistance in *K.*

pneumoniae. Indeed, an absence of phosphoethanolamine modification has been advocated as a way to identify mutational colistin resistance (as opposed to *mcr*-mediated resistance, which does cause this modification) whether due to *mgrB* loss-of-function mutation, PhoPQ activation or PmrAB activation in *K. pneumoniae* (30). Overall, this situation is different from that reported in *Salmonella* spp. (25) and another difference between the species is the finding that PmrE production is constitutive in *K. pneumoniae*, and not part of the PhoPQ or PmrAB regulons (**Figure 5**) which is the case in *Salmonella* spp. (5). In the context of PmrB activation in *K. pneumoniae*, this has also been shown by qRT-PCR (26) and in the context of CrrB activation – leading to PmrAB activation – this has been shown through transcriptomics (20). We confirm here using proteomics that PmrE, which is an enzyme responsible for driving the committed step for the biosynthesis of 4-amino-4-deoxy-L-arabinose required for colistin resistance (5), is present at levels in wild-type cells similar to the levels of Arn protein produced in colistin resistant mutants (**Figures 4, 5**).

Conclusions

Our aim was to definitively investigate the importance of the MgrB-PhoPQ-PmrD-PmrAB signal transduction cascade on Arn and PmrC protein production in *K. pneumoniae*, which has been previously explored using gene knockouts and measurements of transcript levels (5). Based on our data, grounded in protein abundance levels collected during growth in the medium defined for colistin susceptibility testing, we show that this complex interplay, despite remaining potentially important in patients, has minimal importance in the context of colistin resistance in *K. pneumoniae in vitro*. Disruption of *pmrD* or *pmrA* in an *mgrB* loss-of-function mutant does not reduce Arn protein production below a threshold required for colistin resistance (**Figure 3**). Activation of PhoPQ directly or via *mgrB* loss-of-function mutation does not increase the PmrAB-controlled production of PmrC above the level of detection, which is >100-fold less than the observed abundance of PmrC in a PmrB*

activatory mutant (**Figure 5**). Therefore, we conclude that colistin resistance caused by PhoPQ activation in conditions defined for colistin susceptibility testing – i.e. in most clinical cases (28) – is due almost exclusively to PhoPQ activation, leading to Arn protein upregulation, and that the level of Arn protein upregulation dictates colistin MIC during growth. It is interesting to note, therefore that clinical isolates with multiple mutations potentially activating PhoPQ can be found, where there is an additive effect on colistin MIC (28). The implication is that real-world colistin usage in the clinical, in some cases, selects for mutations or combinations of mutations that confer colistin MICs above the currently defined resistance breakpoint.

The reason why other earlier seminal reports have placed far higher importance on the cross-activation of PmrAB by PhoPQ via PmrD (14,18) could be that they used media that caused greater basal activation of PmrAB. It is important to remember that the PmrD linker protein has only experimentally been shown to increase the activation of PmrAB once already activated by an external signal, not to activate it from the basal state (14,18). Since PmrAB activation is affected by iron concentration and pH, it may be that the medium used for colistin susceptibility testing – and used by us here – does not activate PmrAB in the first place, so there is nothing that PmrD can do to enhance activation, effectively silencing the cross-regulatory pathway. Another explanation is that previous work relied on measurements of transcript levels. In some cases, small changes in protein abundance are associated with phenotypically relevant changes in antimicrobial susceptibility, as we have shown previously in *K. pneumoniae*, for example upon loss-of-function mutations in *ramR*, which, despite having <5 fold effects on OmpK35 porin and AcrAB-TolC efflux pump production, has large effects on susceptibility to a range of antimicrobial agents from different classes (31). But in some cases, large changes in gene expression are required to have a phenotypic effect when a gene is not highly expressed in the wild-type, for example in the case of OqxAB efflux pump production as controlled by OqxR in *K. pneumoniae*, which needs to increase >10,000 fold to have a phenotypic effect on resistance (32). One major advantage of

proteomics is that comparisons of protein abundance can be drawn between different gene products, which is not always the case when transcript levels are measured, since the kinetics of DNA hybridisation can have major influences on signal. This advantage is exemplified here, where we confirmed that *pmrE* expression, measured at the level of protein abundance, is not affected by mutations associated with colistin resistance (**Figure 5**). This was also shown by measuring transcript levels (20,24) but the added value of proteomics is that we found that constitutive PmrE protein levels in all backgrounds are similar to those of the Arn proteins following mutation to colistin resistance, rather than constitutive but at low levels (**Figure 5**).

Experimental

Materials, bacterial isolates, selection and generation of mutants

Chemicals were from Sigma and growth media from Oxoid, unless otherwise stated. Strains used were *K. pneumoniae* Ecl8 (30), plus the clinical isolate KP47 (32). To select colistin resistant mutants, one hundred microlitre aliquots of overnight cultures of the parent strain grown in Cation Adjusted Muller-Hinton Broth (CAMHB) were spread onto Mueller-Hinton Agar containing 32 $\mu g.mL^{-1}$ colistin, which were then incubated for 24 h. Insertional inactivation of *phoP*, *pmrD*, or *pmrA* was performed using the pKNOCK suicide plasmid (33). The *phoP*, *pmrD* and *pmrA* DNA fragments were amplified with Phusion High-Fidelity DNA Polymerase (NEB, UK) from *K. pneumoniae* Ecl8 genomic DNA by using primers *phoP* KO FW (5′-AAGCGGACTACTATCTGGGC-3′) and *phoP* KO RV (5′-TGGAAAGGCTTGGTGACGTA-3′); *pmrD* KO FW (5′-AAGTACAGGACAACGCTTCG-3′) and *pmrD* KO RV (5′-AGTTTATCCCCTTCCCGCAG-3′); *pmrA* KO FW (5'-GACGGGCTGCATTTTCTCTC-3') and *pmrA* KO RV (5'-TTACCAGGTAGTCATCCGCC-3'). Each PCR product was ligated into the pKNOCK-GM at the SmaI site. The recombinant plasmid was then transferred into *K. pneumoniae* cells by conjugation. Mutants were

selected for gentamicin non-susceptibility (5 µg.mL^{-1}) and the mutation was confirmed by PCR using primers *phoP* KO RV and BT543 (5'-TGACGCGTCCTCGGTAC-3'); *pmrD* KO FW and BT543; *pmrA* KO RV and BT543.

Determining minimal inhibitory concentrations (MICs) of colistin

MICs were determined using CLSI broth microtitre assays (34) and interpreted using published breakpoints (35). Briefly, a PBS bacterial suspension was prepared to obtain a stock of OD_{600}=0.01. The final volume in each well of a 96-well cell culture plate (Corning Costar) was 200 µL and included 20 µL of the bacterial suspension. Bacterial growth was determined after 20 h of incubation by measuring OD_{600} values using a POLARstar Omega spectrophotometer (BMG Labtech).

Proteomics

500 µL of an overnight CAMHB culture were transferred to 50 mL CAMHB and cells were grown at 37˚C to 0.6 OD_{600}. Cells were pelleted by centrifugation (10 min, 4,000 × *g*, 4°C) and resuspended in 30 mL of 30 mM Tris-HCl, pH 8 and broken by sonication using a cycle of 1 s on, 0.5 s off for 3 min at amplitude of 63% using a Sonics Vibracell VC-505TM (Sonics and Materials Inc., Newton, Connecticut, USA). The sonicated samples were centrifuged at 8,000 rpm (Sorval RC5B PLUS using an SS-34 rotor) for 15 min at 4°C to pellet intact cells and large cell debris. For envelope preparations, the supernatant was subjected to centrifugation at 20,000 rpm for 60 min at 4°C using the above rotor to pellet total envelopes. To isolate total envelope proteins, this total envelope pellet was solubilised using 200 µL of 30 mM Tris-HCl pH 8 containing 0.5% (w/v) SDS.

Protein concentrations in all samples were quantified using Biorad Protein Assay Dye Reagent Concentrate according to the manufacturer's instructions. Proteins (2.5 µg/lane)

were separated by SDS-PAGE using 11% acrylamide, 0.5% bis-acrylamide (Biorad) gels and a Biorad Min-Protein Tetracell chamber model 3000X1. Gels were resolved at 175 V until the dye front had moved approximately 1 cm into the separating gel. Proteins in all gels were stained with Instant Blue (Expedeon) for 10 min and de-stained in water.

The 1 cm of gel lane was subjected to in-gel tryptic digestion using a DigestPro automated digestion unit (Intavis Ltd). The resulting peptides from each gel fragment were fractionated separately using an Ultimate 3000 nanoHPLC system in line with an LTQ-Orbitrap Velos mass spectrometer (Thermo Scientific). In brief, peptides in 1% (v/v) formic acid were injected onto an Acclaim PepMap C18 nano-trap column (Thermo Scientific). After washing with 0.5% (v/v) acetonitrile plus 0.1% (v/v) formic acid, peptides were resolved on a 250 mm × 75 µm Acclaim PepMap C18 reverse phase analytical column (Thermo Scientific) over a 150 min organic gradient, using 7 gradient segments (1-6% solvent B over 1 min, 6-15% B over 58 min, 15-32% B over 58 min, 32-40% B over 5 min, 40-90% B over 1 min, held at 90% B for 6 min and then reduced to 1% B over 1 min) with a flow rate of 300 nL/min. Solvent A was 0.1% formic acid and Solvent B was aqueous 80% acetonitrile in 0.1% formic acid. Peptides were ionized by nano-electrospray ionization MS at 2.1 kV using a stainless-steel emitter with an internal diameter of 30 µm (Thermo Scientific) and a capillary temperature of 250°C. Tandem mass spectra were acquired using an LTQ-Orbitrap Velos mass spectrometer controlled by Xcalibur 2.1 software (Thermo Scientific) and operated in data-dependent acquisition mode. The Orbitrap was set to analyse the survey scans at 60,000 resolution (at m/z 400) in the mass range m/z 300 to 2000 and the top twenty multiply charged ions in each duty cycle selected for MS/MS in the LTQ linear ion trap. Charge state filtering, where unassigned precursor ions were not selected for fragmentation, and dynamic exclusion (repeat count, 1; repeat duration, 30 s; exclusion list size, 500) were used. Fragmentation conditions in the LTQ were as follows: normalized collision energy, 40%; activation q, 0.25; activation time 10 ms; and minimum ion selection intensity, 500 counts.

354 The raw data files were processed and quantified using Proteome Discoverer software v1.4
355 (Thermo Scientific) and searched against the UniProt *K. pneumoniae* strain ATCC 700721 /
356 MGH 78578 database (5126 protein entries; UniProt accession 272620) using the
357 SEQUEST algorithm. Peptide precursor mass tolerance was set at 10 ppm, and MS/MS
358 tolerance was set at 0.8 Da. Search criteria included carbamidomethylation of cysteine
359 (+57.0214) as a fixed modification and oxidation of methionine (+15.9949) as a variable
360 modification. Searches were performed with full tryptic digestion and a maximum of 1 missed
361 cleavage was allowed. The reverse database search option was enabled, and all peptide
362 data was filtered to satisfy false discovery rate (FDR) of 5 %. Protein abundance
363 measurements were calculated from peptide peak areas using the Top 3 method (36) and
364 proteins with fewer than three peptides identified were excluded. The proteomic analysis
365 was repeated three times for each parent and mutant strain, each using a separate batch of
366 cells. Specific protein abundance was normalised based on the average abundance of the
367 50 most abundant proteins in each sample. Comparisons of normalised abundance between
368 samples used an unpaired t-test, and significance was defined with $p < 0.05$. Fold-change in
369 abundance between strains was calculated by first calculating average normalised
370 abundance across the three samples representing each strain.

371

372 *Whole genome sequencing to identify mutations*

373 Whole genome resequencing was performed by MicrobesNG (Birmingham, UK) on a HiSeq
374 2500 instrument (Illumina, San Diego, CA, USA). Reads were trimmed using Trimmomatic
375 (37) and assembled into contigs using SPAdes 3.10.1 (http://cab.spbu.ru/software/spades/).
376 Assembled contigs were mapped to the *K. pneumoniae* Ecl8 reference genome (GenBank
377 accession number GCF_000315385.1), obtained from GenBank by using progressive
378 Mauve alignment software (38).

379

Acknowledgments

This work was funded by grant MR/S004769/1 to M.B.A. from the Antimicrobial Resistance Cross Council Initiative supported by the seven United Kingdom research councils and the National Institute for Health Research. Genome sequencing was provided by MicrobesNG (http://www.microbesng.uk/), which is supported by the BBSRC (grant number BB/L024209/1).

We declare no conflicts of interest.

Figure Legends

Figure 1. Sequence at the 5' end of *mgrB* and upstream in colistin resistant mutant P22.

The two promoters for *mgrB* are highlighted in blue and green. The mutation in P22 alters the wild-type sequence at the position highlighted in yellow from A to G in the putative -10 box of the second promoter, which is marked with two stars. The first promoter sequence, defined as -35 and -10 was defined in (10).

Figure 2. Arn protein abundance in parent strain Ecl8 versus three *mgrB* mutants.

Strains were grown in CAMHB and raw envelope protein abundance data for each Arn protein in a sample are presented normalised using the average abundance of the 50 most abundant proteins in that sample. Data for three biological replicates of parent (Ecl8) and *mgrB* mutants (P21, P22 and P23) are presented as mean +/- Standard Error of the Mean. All mutants have statistically significantly increased production of all Arn proteins relative to Ecl8 based on a t-test ($p<0.05$).

Figure 3. Arn protein abundance in *mgrB* loss-of-function mutant P23 versus its *phoP*. *pmrD* and *pmrA* loss-of-function mutant derivatives.

Strains were grown in CAMHB and raw envelope protein abundance data for each Arn protein in a sample are presented normalised using the average abundance of the 50 most abundant proteins in that sample. Data for three biological replicates of parent (P23) and mutants where *phoP*, *pmrD* or *pmrA* had been insertionally inactivated (PhoP-, PmrD- or PmrA-) are presented as mean +/- Standard Error of the Mean. All PhoP- mutants have statistically significantly reductions in production of all Arn proteins relative to P23 based on

412 a t-test ($p<0.05$). For PmrD- and PmrA- mutants, significant changes relative to P23 are
413 noted with a star.

414 **Figure 4. Arn protein abundance in *mgrB* mutant P23 versus clinical isolate KP47 and**
415 **PhoQ* or PmrB* (activatory) mutant derivatives.**

416 Strains were grown in CAMHB and raw envelope protein abundance data for each Arn
417 protein in a sample are presented normalised using the average abundance of the 50 most
418 abundant proteins in that sample. Data for three biological replicates of parent (KP47) and
419 mutants where PhoQ or PmrA have been activated, compared with the *mgrB* loss-of-function
420 mutant P23 are presented as mean +/- Standard Error of the Mean. All Arn proteins, and all
421 Arn proteins except ArnB are significantly upregulated relative to KP47 in its PhoQ* mutant,
422 and PmrB* mutant, respectively based on a t-test ($p<0.05$). For the PmrB* mutant,
423 significantly lower abundances relative to the PhoQ* mutant are noted with a star.

424

425 **Figure 5. PmrA, B, C and E protein abundance in *mgrB* mutant P23 versus clinical**
426 **isolate KP47 and PhoQ* or PmrB* (activatory) mutant derivatives.**

427 Strains were grown in CAMHB and raw envelope protein abundance data for each Pmr
428 protein in a sample are presented normalised using the average abundance of the 50 most
429 abundant proteins in that sample. Data for three biological replicates of parent (KP47) and
430 mutants where PhoQ or PmrA have been activated, compared with the *mgrB* loss-of-function
431 mutant P23 are presented as mean +/- Standard Error of the Mean. PmrA, B and C were
432 significantly upregulated relative to KP47 in its PmrB* mutant based on a t-test ($p<0.05$). No
433 other differences were statistically significant.

434

Tables

Table 1: MICs of colistin against clinical isolates and mutant derivatives.

Strain/ mutant	Colistin MIC (µg.mL^{-1})
Ecl8	1
P21 (*mgrB*)	64
P22 (*mgrB*)	32
P23 (*mgrB*)	128
P23 *phoP*	2
P23 *pmrD*	64
P23 *pmrA*	64
KP47	2
KP47 PhoQ*	64
KP47 PmrB*	32

Values reported are the modes of three repetitions. Shading indicates resistance according to susceptibility breakpoints set by the CLSI (35).

Table 2: Significant changes in envelope protein abundance seen in *K. pneumoniae mgrB* mutant P21 versus parent strain Ecl8

Strains were grown in CAMHB and raw abundance data for each protein in a sample are presented normalised using the average abundance of the 50 most abundant proteins in that sample. Data for three biological replicates of parent (Ecl8) and *mgrB* mutant (P21). Proteins listed are those significantly differently up- (fold change >1) or down-regulated (fold change <1) in P21, and in *mgrB* mutants P22 and P23 versus their parent Ecl8, based on t-test. Shading indicates proteins also upregulated in the PmrB* (activatory) mutant of *K. pneumoniae* clinical isolate KP47 relative to KP47, see text. Stars indicate proteins encoded by transcripts upregulated in a *K. pneumoniae* CrrB activatory mutant (20).

Accession	Description	Ecl8 1	Ecl8 2	Ecl8 3	P21 1	P21 2	P21 3	Fold Change	t-test
A6T5Y8	Mg2+ transport ATPase	0.01	0.00	0.00	0.02	0.04	0.03	7.63	0.01
A6T7F8	Thymidylate kinase	0.01	0.00	0.00	0.01	0.02	0.01	4.29	0.02
A6TBQ4	Lipid A 1-diphosphate synthase	0.00	0.00	0.00	0.07	0.09	0.08	>100	0.00
A6THT5	Putative porin	0.01	0.02	0.00	0.16	0.16	0.08	13.77	0.01
A6T4W9	Bifunctional uridylyltransferase/ uridylyl-removing enzyme	0.00	0.00	0.00	0.01	0.01	0.00	2.76	0.04
A6T5U9	Putative periplasmic binding protein	0.00	0.00	0.00	0.01	0.02	0.01	>100	<0.005
A6THH1	MgtA	0.00	0.00	0.00	0.01	0.03	0.02	>100	<0.005
A6T6X6	MacA	0.00	0.00	0.00	0.01	0.02	0.02	11.68	0.01
A6T7D1	Hypothetical Protein	0.01	0.00	0.01	0.01	0.01	0.01	1.83	0.03
A6T7J8	PhoP	0.01	0.01	0.01	0.05	0.06	0.05	5.41	<0.005
A6T9Y9	SlyB	0.37	0.38	0.17	0.81	1.04	0.46	2.52	0.03
A6TBT1	AbpE	0.00	0.01	0.00	0.01	0.03	0.01	5.61	0.02
A6TCT2	LpxO	0.01	0.01	0.01	0.03	0.04	0.02	4.77	0.01
A6TF96	ArnT	0.00	0.00	0.00	0.02	0.01	0.01	>100	<0.005
A6TF97	ArnD	0.00	0.00	0.00	0.03	0.04	0.02	>100	<0.005
A6TF98	ArnA	0.01	0.00	0.00	0.09	0.11	0.15	20.27	<0.005
A6TF99	ArnC	0.00	0.00	0.00	0.05	0.08	0.05	>100	<0.005
A6TFA0	ArnB	0.00	0.00	0.00	0.05	0.00	0.04	>100	0.04
A6T7H3	Putative enzyme	0.01	0.01	0.01	0.01	0.01	0.01	1.67	0.04
A6TEP0	Cell division protein ZapE	0.02	0.01	0.01	0.05	0.04	0.02	2.36	0.03
A6T6G3	Tol-Pal system protein TolQ	0.04	0.04	0.03	0.06	0.08	0.05	1.73	0.04
A6TDS9	Component of the MscS	0.06	0.03	0.04	0.06	0.09	0.07	1.65	0.04

	mechanosensitive channel								
A6T4X0	Methionine aminopeptidase	0.04	0.04	0.05	0.06	0.05	0.05	1.29	0.01
A6T5I4	Peptidylprolyl isomerase	0.13	0.07	0.09	0.20	0.18	0.21	2.00	<0.005
A6T642	2,3-dihydro-2,3-dihydroxybenzoate synthetase, isochroismatase	0.00	0.00	0.01	0.01	0.01	0.01	2.17	0.03
A6T7K1	Adenylosuccinate lyase	0.16	0.09	0.12	0.16	0.22	0.17	1.47	0.05
A6T7R3	Putative chitinase II	0.02	0.03	0.02	0.02	0.01	0.02	0.69	0.01
A6T7X8	Cob(I)yrinic acid a,c-diamide adenosyltransferase	0.01	0.01	0.01	0.01	0.02	0.01	1.75	0.05
A6T9L3	Alcohol dehydrogenase	0.04	0.04	0.08	0.02	0.02	0.01	0.35	0.03
A6T9V4	Glucans biosynthesis protein D	0.02	0.01	0.01	0.00	0.00	0.01	0.27	0.03
A6TA04	Superoxide dismutase	0.03	0.02	0.04	0.01	0.00	0.00	0.14	0.01
A6TAU7	Probable formate acetyltransferase 3	0.28	0.25	0.28	0.19	0.25	0.23	0.83	0.04
A6TCB4	Phosphoribosylglycinamide formyltransferase	0.03	0.02	0.02	0.03	0.04	0.03	1.55	0.01
A6TCL8	Signal recognition particle protein	0.05	0.03	0.04	0.06	0.06	0.06	1.51	0.01
A6TD49	CysJ	0.03	0.02	0.02	0.00	0.00	0.00	<0.01	<0.005
A6TE01	Uncharacterized protein	0.02	0.01	0.02	0.02	0.02	0.02	1.35	0.03
A6TEB4	3-hydroxy-5-phosphonooxypentane-2,4-dione thiolase	0.02	0.02	0.03	0.01	0.01	0.01	0.46	0.03
A6TEE8	2-hydroxy-3-oxopropionate reductase	0.01	0.01	0.02	0.00	0.00	0.00	<0.01	0.01
A6TEZ6	Cyclic AMP receptor protein	0.45	0.32	0.26	0.47	0.47	0.54	1.44	0.03
A6TF07	CysG2	0.01	0.01	0.01	0.01	0.01	0.01	0.73	0.02
A6TFY4	Putative glycoside hydrolase	0.00	0.00	0.01	0.00	0.00	0.00	0.24	0.03
A6TGM2	NAD(P)H-flavin reductase	0.06	0.05	0.05	0.08	0.08	0.08	1.54	0.01
A6TGU4	MalE	0.02	0.01	0.02	0.00	0.01	0.00	0.32	0.04
A6TGU6	LamB2	0.30	0.28	0.41	0.18	0.22	0.26	0.67	0.04
A6THU9	4-hydroxyphenylacetate catabolism	0.01	0.01	0.01	0.02	0.02	0.02	2.57	<0.005

462

463 **Table 3: Significant changes in envelope protein abundance seen in *K. pneumoniae* mutant P23 *phoP* versus P23**

Strains were grown in CAMHB and raw abundance data for each protein in a sample are presented normalised using the average abundance of the 50 most abundant proteins in that sample. Data for three biological replicates of colistin resistant *mgrB* mutant P23 and its *phoP* insertionally inactivated derivative. Proteins listed are those significantly (based on t-test) differently up- (fold change >1) or down-regulated (fold change <1) in P23 *phoP* versus P23; considering only proteins that were oppositely regulated in P23 compared with its colistin susceptible parent, Ecl8, as listed in **Table 2**. Shading indicates proteins not upregulated in the PhoQ* (activatory) mutant of *K. pneumoniae* clinical isolate KP47 relative to KP47; the other 15/18 proteins not shaded are therefore considered the core PhoPQ regulon, see text. Stars indicate proteins encoded by transcripts upregulated in a *K. pneumoniae* PhoQ activatory mutant (20).

Accession	**Description**	**P23 1**	**P23 2**	**P23 3**	***phoP* 1**	***phoP* 2**	***phoP* 3**	**Fold Change**	**t-test**
A6T4W9	GlnD	0.005	0.011	0.009	0.005	0.002	0.003	0.408	0.027
A6T5U9	Putative periplasmic binding protein	0.036	0.029	0.024	0.000	0.000	0.000	<0.01	0.001
A6T5Y8	Mg2+ transport ATPase*	0.033	0.041	0.032	0.002	0.000	0.000	0.018	<0.005
A6T6X6	MacA*	0.016	0.024	0.021	0.006	0.010	0.002	0.305	0.005
A6T7D1	Hypothetical Protein	0.017	0.021	0.022	0.016	0.014	0.013	0.714	0.019
A6T7F8	Thymidylate kinase	0.021	0.018	0.016	0.016	0.013	0.011	0.740	0.039
A6T7J8	PhoP*	0.087	0.105	0.125	0.011	0.000	0.000	0.036	<0.005
A6T9Y9	SlyB*	1.833	2.191	1.513	0.669	0.634	0.697	0.361	0.002
A6TBQ4	Lipid A 1-diphosphate synthase	0.122	0.153	0.122	0.012	0.000	0.000	0.030	<0.005
A6TBT1	ApbE*	0.043	0.045	0.038	0.014	0.005	0.005	0.189	<0.005
A6TCT2	LpxO*	0.048	0.052	0.037	0.009	0.000	0.003	0.081	0.001
A6TF96	ArnT*	0.040	0.070	0.035	0.000	0.000	0.000	<0.01	0.006
A6TF97	ArnD*	0.071	0.041	0.041	0.000	0.000	0.000	<0.01	0.004
A6TF98	ArnA*	0.496	0.309	0.321	0.000	0.000	0.000	<0.01	<0.005
A6TF99	ArnC*	0.236	0.313	0.247	0.000	0.000	0.000	<0.01	<0.005
A6TFA0	ArnB*	0.098	0.051	0.053	0.000	0.000	0.000	<0.01	0.006
A6THH1	MgtA*	0.025	0.036	0.031	0.000	0.000	0.000	<0.01	<0.005
A6THT5	Putative porin	0.639	0.794	0.614	0.053	0.054	0.058	0.081	<0.005

Figures

Figure 1

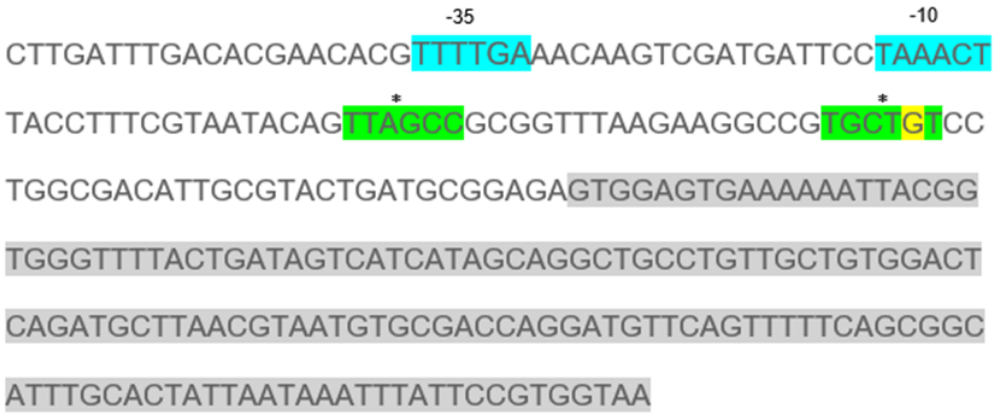

477 **Figure 2**

478

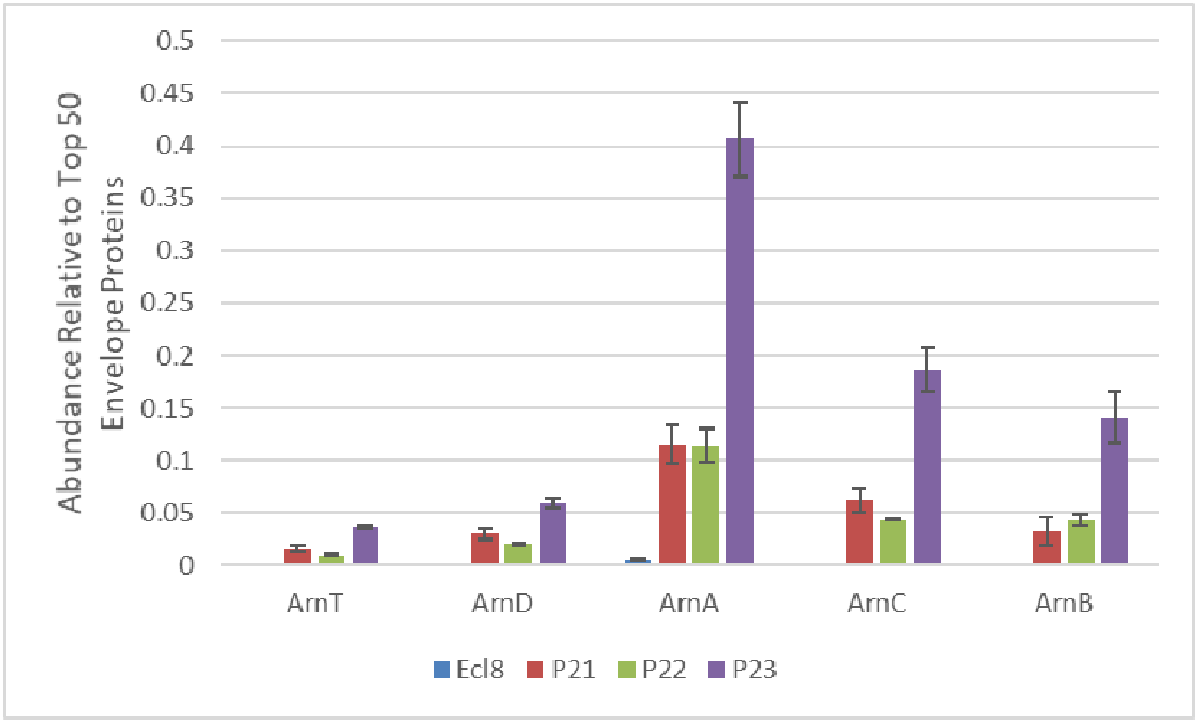

479
480

481 **Figure 3**

482

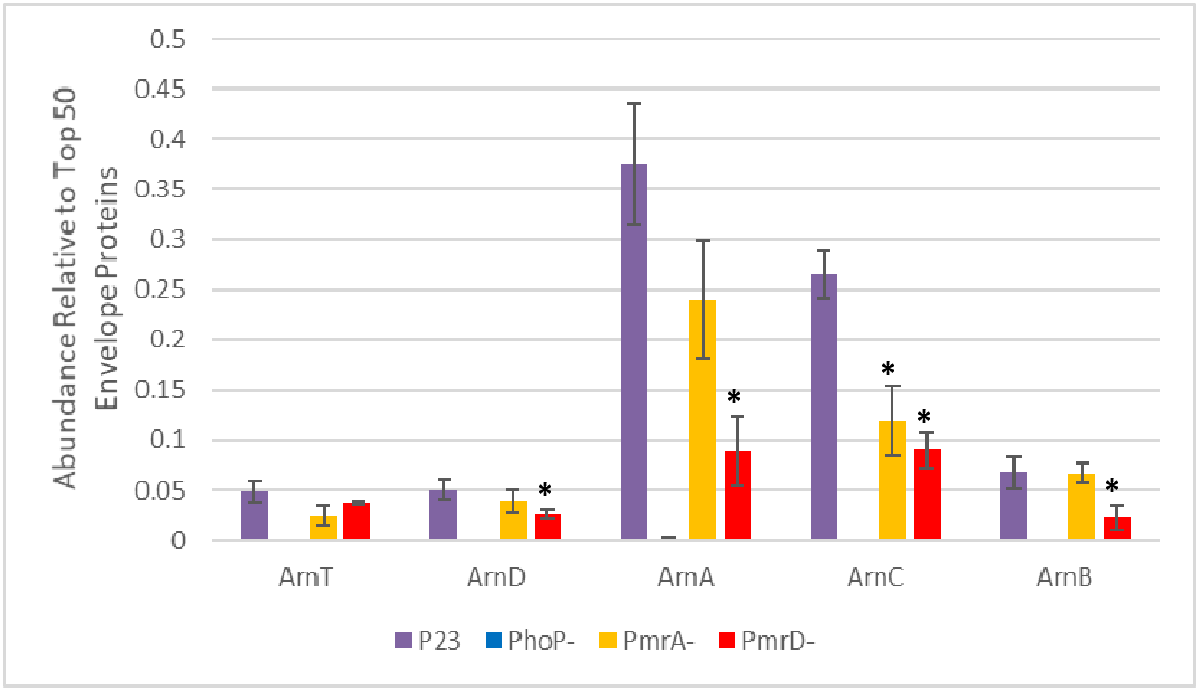

483
484

485 **Figure 4**

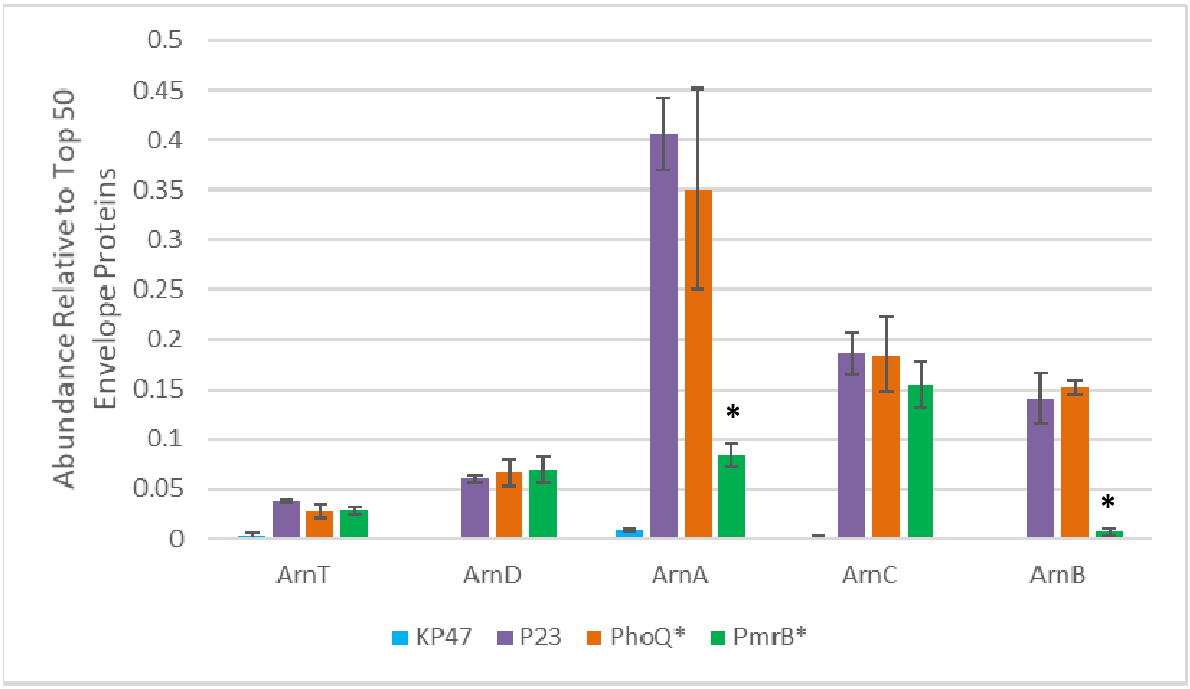

494 **Figure 5**

495

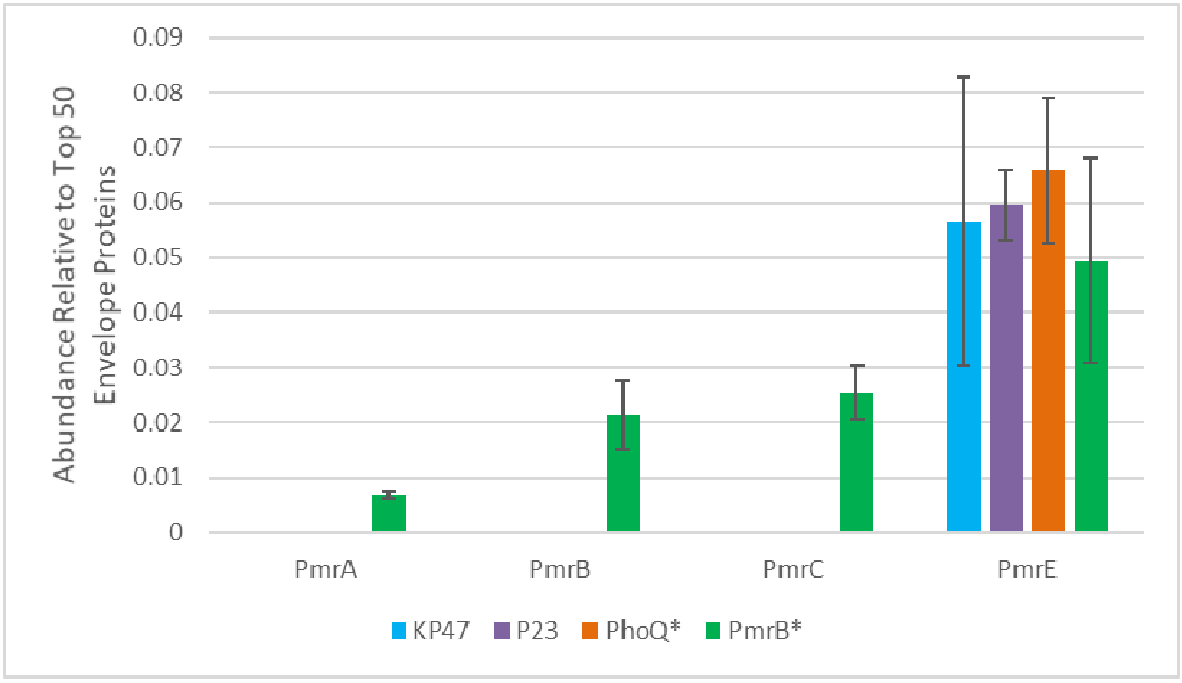

496
497

References

1. Durante-Mangoni E, Andini R, Zampino R. Management of carbapenem-resistant Enterobacteriaceae infections. Clin Microbiol Infect. 2019 25:943-950.
2. Tóth A, Damjanova I, Puskás E, Jánvári L, Farkas M, Dobák A, Böröcz K, Pászti J. Emergence of a colistin-resistant KPC-2-producing Klebsiella pneumoniae ST258 clone in Hungary. Eur J Clin Microbiol Infect Dis. 2010 Jul;29(7):765-9. doi: 10.1007/s10096-010-0921-3. Epub 2010 Apr 18.
3. Kontopoulou K, Protonotariou E, Vasilakos K, Kriti M, Koteli A, Antoniadou E, Sofianou D. Hospital outbreak caused by Klebsiella pneumoniae producing KPC-2 beta-lactamase resistant to colistin. J Hosp Infect. 2010 Sep;76(1):70-3. doi: 10.1016/j.jhin.2010.03.021. Epub 2010 Jun 17.
4. Elemam A, Rahimian J, Doymaz M. In vitro evaluation of antibiotic synergy for polymyxin B-resistant carbapenemase-producing Klebsiella pneumoniae. J Clin Microbiol. 2010 Oct;48(10):3558-62. doi: 10.1128/JCM.01106-10. Epub 2010 Aug 4.
5. Jeannot K, Bolard A, Plésiat P. Resistance to polymyxins in Gram-negative organisms. Int J Antimicrob Agents. 2017 May;49(5):526-535.
6. Deshpande LM, Hubler C, Davis AP, Castanheira M. Updated Prevalence of mcr-Like Genes among Escherichia coli and Klebsiella pneumoniae in the SENTRY Program and Characterization of mcr-1.11 Variant. Antimicrob Agents Chemother. 2019 Mar 27;63(4). pii: e02450-18.
7. Cannatelli A, D'Andrea MM, Giani T, Di Pilato V, Arena F, Ambretti S, Gaibani P, Rossolini GM. In vivo emergence of colistin resistance in Klebsiella pneumoniae producing KPC-type carbapenemases mediated by insertional inactivation of the PhoQ/PhoP mgrB regulator. Antimicrob Agents Chemother. 2013 Nov;57(11):5521-6.
8. López-Camacho E, Gómez-Gil R, Tobes R, Manrique M, Lorenzo M, Galván B, Salvarelli E, Moatassim Y, Salanueva IJ, Pareja E, Codoñer FM, Alvarez-Tejado M, Garcillán-Barcia MP, De la Cruz F, Mingorance J. Genomic analysis of the emergence and

525 evolution of multidrug resistance during a Klebsiella pneumoniae outbreak including
526 carbapenem and colistin resistance. J Antimicrob Chemother. 2014 Mar;69(3):632-6.
527 9. Cannatelli A, Giani T, D'Andrea MM, Di Pilato V, Arena F, Conte V, Tryfinopoulou K,
528 Vatopoulos A, Rossolini GM; COLGRIT Study Group. MgrB inactivation is a common
529 mechanism of colistin resistance in KPC-producing Klebsiella pneumoniae of clinical
530 origin. Antimicrob Agents Chemother. 2014 Oct;58(10):5696-703.
531 10. Poirel L, Jayol A, Bontron S, Villegas MV, Ozdamar M, Türkoglu S, Nordmann P. The
532 mgrB gene as a key target for acquired resistance to colistin in Klebsiella pneumoniae. J
533 Antimicrob Chemother. 2015 Jan;70(1):75-80.
534 11. Helander IM, Kato Y, Kilpeläinen I, Kostiainen R, Lindner B, Nummila K, Sugiyama T,
535 Yokochi T. Characterization of lipopolysaccharides of polymyxin-resistant and polymyxin-
536 sensitive Klebsiella pneumoniae O3. Eur J Biochem. 1996 Apr 1;237(1):272-8.
537 12. Leung LM, Cooper VS, Rasko DA, Guo Q, Pacey MP, McElheny CL, Mettus RT, Yoon
538 SH, Goodlett DR, Ernst RK, Doi Y. Structural modification of LPS in colistin-resistant,
539 KPC-producing Klebsiella pneumoniae. J Antimicrob Chemother. 2017 Nov
540 1;72(11):3035-3042.
541 13. Jasim R, Baker MA, Zhu Y, Han M, Schneider-Futschik EK, Hussein M, Hoyer D, Li J,
542 Velkov T. A Comparative Study of Outer Membrane Proteome between Paired Colistin-
543 Susceptible and Extremely Colistin-Resistant Klebsiella pneumoniae Strains. ACS Infect
544 Dis. 2018 Dec 14;4(12):1692-1704.
545 14. Mitrophanov AY, Jewett MW, Hadley TJ, Groisman EA. Evolution and dynamics of
546 regulatory architectures controlling polymyxin B resistance in enteric bacteria. PLoS
547 Genet. 2008 Oct;4(10):e1000233.
548 15. Humphries RM, Green DA, Schuetz AN, Bergman Y, Lewis S, Yee R, Stump S, Lopez
549 M, Macesic N, Uhlemann AC, Kohner P, Cole N, Simner PJ. Multicenter Evaluation of
550 Colistin Broth Disk Elution and Colistin Agar Test: a Report from the Clinical and
551 Laboratory Standards Institute. J Clin Microbiol. 2019 Oct 23;57(11). pii: e01269-19.
552 16. Carretto E, Brovarone F, Russello G, Nardini P, El-Bouseary MM, Aboklaish AF, Walsh

553 TR, Tyrrell JM. Clinical Validation of SensiTest Colistin, a Broth Microdilution-Based
554 Method To Evaluate Colistin MICs. J Clin Microbiol. 2018 Mar 26;56(4). pii: e01523-17.
555 17. CLSI-EUCAST Polymyxin Breakpoints Working Group. 2016. Recommendations for MIC
556 determination of colistin (polymyxin E) as recommended by the joint CLSI-EUCAST
557 Polymyxin Breakpoints Working Group. EUCAST
558 http://www.eucast.org/fileadmin/src/media/PDFs/EUCAST_files/General_documents/Rec
559 ommendations_for_MIC_determination_of_colistin_March_2016.pdf.
560 18. Cheng HY, Chen YF, Peng HL. Molecular characterization of the PhoPQ-PmrD-PmrAB
561 mediated pathway regulating polymyxin B resistance in Klebsiella pneumoniae CG43. J
562 Biomed Sci. 2010 Jul 24;17:60
563 19. Lippa AM, Goulian M. Feedback inhibition in the PhoQ/PhoP signaling system by a
564 membrane peptide, PLoS Genet, 2009, 5: e1000788.
565 20. Wright MS, Suzuki Y, Jones MB, Marshall SH, Rudin SD, van Duin D, Kaye K, Jacobs
566 MR, Bonomo RA, Adams MD. Genomic and transcriptomic analyses of colistin-resistant
567 clinical isolates of Klebsiella pneumoniae reveal multiple pathways of resistance.
568 Antimicrob Agents Chemother. 2015 Jan;59(1):536-43.
569 21. Halaby T, Kucukkose E, Janssen AB, Rogers MR, Doorduijn DJ, van der Zanden AG, Al
570 Naiemi N, Vandenbroucke-Grauls CM, van Schaik W. Genomic Characterization of
571 Colistin Heteroresistance in Klebsiella pneumoniae during a Nosocomial Outbreak.
572 Antimicrob Agents Chemother. 2016 Oct 21;60(11):6837-6843.
573 22. Jayol A, Nordmann P, Brink A, Poirel L. Heteroresistance to colistin in Klebsiella
574 pneumoniae associated with alterations in the PhoPQ regulatory system. Antimicrob
575 Agents Chemother. 2015 May;59(5):2780-4.
576 23. Cannatelli A, Di Pilato V, Giani T, Arena F, Ambretti S, Gaibani P, D'Andrea MM,
577 Rossolini GM. In vivo evolution to colistin resistance by PmrB sensor kinase mutation in
578 KPC-producing Klebsiella pneumoniae is associated with low-dosage colistin treatment.
579 Antimicrob Agents Chemother. 2014 Aug;58(8):4399-403.
580 24. Jayol A, Poirel L, Brink A, Villegas MV, Yilmaz M, Nordmann P. Resistance to colistin

associated with a single amino acid change in protein PmrB among Klebsiella pneumoniae isolates of worldwide origin. Antimicrob Agents Chemother. 2014 Aug;58(8):4762-6.

25. Lee H, Hsu FF, Turk J, Groisman EA. The PmrA-regulated pmrC gene mediates phosphoethanolamine modification of lipid A and polymyxin resistance in Salmonella enterica. J Bacteriol. 2004 Jul;186(13):4124-33.
26. Cheng YH, Lin TL, Lin YT, Wang JT. Amino Acid Substitutions of CrrB Responsible for Resistance to Colistin through CrrC in Klebsiella pneumoniae. Antimicrob Agents Chemother. 2016 May 23;60(6):3709-16.
27. Jayol A, Nordmann P, Brink A, Villegas MV, Dubois V, Poirel L. High-Level Resistance to Colistin Mediated by Various Mutations in the crrB Gene among Carbapenemase-Producing Klebsiella pneumoniae. Antimicrob Agents Chemother. 2017 Oct 24;61(11). pii: e01423-17.
28. Macesic N, Nelson B, Mcconville TH, Giddins MJ, Green DA, Stump S, Gomez-Simmonds A, Annavajhala MK, Uhlemann AC. Emergence of Polymyxin Resistance in Clinical Klebsiella pneumoniae Through Diverse Genetic Adaptations: A Genomic, Retrospective Cohort Study. Clin Infect Dis. pii: ciz623. doi: 10.1093/cid/ciz623. [Epub ahead of print]
29. Kidd TJ, Mills G, Sá-Pessoa J, Dumigan A, Frank CG, Insua JL, Ingram R, Hobley L, Bengoechea JA. A Klebsiella pneumoniae antibiotic resistance mechanism that subdues host defences and promotes virulence. EMBO Mol Med. 2017 9:430-447.
30. Jiménez-Castellanos JC, Wan Nur Ismah WAK, Takebayashi Y, Findlay J, Schneiders T, Heesom KJ, Avison MB. Envelope proteome changes driven by RamA overproduction in Klebsiella pneumoniae that enhance acquired β-lactam resistance. J Antimicrob Chemother. 2018 73:88-94.
31. Wan Nur Ismah WAK, Takebayashi Y, Findlay J, Heesom KJ, Avison MB. Impact of OqxR loss of function on the envelope proteome of Klebsiella pneumoniae and susceptibility to antimicrobials. J Antimicrob Chemother. 2018 73:2990-2996.

609 32. Wan Nur Ismah WAK, Takebayashi Y, Findlay J, Heesom KJ, Jiménez-Castellanos JC,
610 Zhang J, Graham L, Bowker K, Williams OM, MacGowan AP, Avison MB. 2018.
611 Prediction of Fluoroquinolone Susceptibility Directly from Whole-Genome Sequence
612 Data by Using Liquid Chromatography-Tandem Mass Spectrometry To Identify Mutant
613 Genotypes. Antimicrob Agents Chemother 62 pii:e01814-17.
614 33. Alexeyev MF. 1999. The pKNOCK series of broad-host-range mobilizable suicide
615 vectors for gene knockout and targeted DNA insertion into the chromosome of gram-
616 negative bacteria. BioTechniques 26:824-828.
617 34. Clinical and Laboratory Standards Institute. 2015. M07-A10. Methods for dilution
618 antimicrobial susceptibility tests for bacteria that grow aerobically; approved standard,
619 10th ed. Clinical and Laboratory Standards Institute, Wayne, PA.
620 35. Clinical and Laboratory Standards Institute. 2019. M100-S29. Performance standards for
621 antimicrobial susceptibility testing; twenty-ninth informational supplement. An
622 informational supplement for global application developed through the Clinical and
623 Laboratory Standards Institute consensus process. Clinical and Laboratory Standards
624 Institute, Wayne, PA.
625 36. Silva JC, Gorenstein MV, Li G-Z, Vissers JPC, Geromanos SJ. 2006. Absolute
626 quantification of proteins by LCMSE: a virtue of parallel MS acquisition. Mol Cell
627 Proteomics 5:144–156.
628 37. Bolger AM, Lohse M, Usadel B. 2014. Trimmomatic: a flexible trimmer for Illumina
629 sequence data. Bioinformatics 30:2114–2120.
630 38. Darling AE, Mau B, Perna NT, Batzoglou S, Zhong Y. 2010. progressiveMauve: multiple
631 genome alignment with gene gain, loss and rearrangement. PLoS One 5:e11147.